

See discussions, stats, and author profiles for this publication at: <https://www.researchgate.net/publication/275098271>

Enhanced Precombustion Capture of Carbon Dioxide by Gas Hydrate Formation in Water-in-Oil Emulsions

ARTICLE *in* ENERGY & FUELS · APRIL 2015

Impact Factor: 2.79 · DOI: 10.1021/acs.energyfuels.5b00051

READS

22

1 AUTHOR:



[Dongliang Zhong](#)

Chongqing University

21 PUBLICATIONS 153 CITATIONS

SEE PROFILE

Enhanced Precombustion Capture of Carbon Dioxide by Gas Hydrate Formation in Water-in-Oil Emulsions

Kun Ding,[†] Dong-Liang Zhong,^{*,†,‡} Yi-Yu Lu,[‡] and Jia-Le Wang[†]

[†]Key Laboratory of Low-Grade Energy Utilization Technologies and Systems, Ministry of Education of China, Chongqing University, Chongqing 400044, China

[‡]State Key Laboratory of Coal Mine Disaster Dynamics and Control, Chongqing University, Chongqing 400044, China

ABSTRACT: In this work, we reported enhanced kinetics of gas hydrate formation in water-in-oil (W/O) emulsions for the precombustion capture of carbon dioxide. The experiments were carried out at 274.2 K and in the pressure range of 3.0–6.0 MPa. The parameters of induction time, gas uptake, rate of hydrate growth, CO₂ recovery, and separation factor were determined to evaluate the performance of the W/O emulsions for CO₂ capture from a fuel gas (40 mol % CO₂/H₂). It was found that shorter induction time and higher gas uptake were obtained while the water–oil volume ratio (WOR) was reduced from 70% to 20%, and gas hydrates were observed to grow faster at low WORs. The CO₂ recovery and CO₂ concentration in the hydrate phase decreased with WOR decreasing from 70% to 20%. At a fixed WOR, higher pressure resulted in shorter induction time and higher gas uptake, but CO₂ concentration in the hydrate phase decreased. The highest value of CO₂ concentration in the hydrate phase achieved 84 mol % at 3.0 MPa and WOR = 70%, and the highest value of gas uptake obtained in W/O emulsions was 39.5 mmol of gas/mol of water at 3.0 MPa and WOR = 20%. This gas uptake was much higher than that obtained in stirred reactors in the presence of CP or THF and was comparable with that obtained in the fixed bed of silica sand in the presence of THF or TBAB. The result indicated that the W/O emulsions employed in this work are a viable option to enhance hydrate formation for the precombustion capture of carbon dioxide.

1. INTRODUCTION

The emission of carbon dioxide (CO₂) due to the combustion of fossil fuels (coal, oil, and natural gas) has been identified as the major contribution to the release of greenhouse gas and subsequent global warming and climate change.¹ Power plants that burn fossil fuels are known to produce approximately one-third of the total CO₂ emission per year. Therefore, reducing CO₂ emission of these power plants is strongly required.^{2–5} Precombustion capture, oxy-fuel combustion, and postcombustion capture are three approaches available for power plants to capture CO₂.⁶ Oxy-fuel combustion and postcombustion capture refer to CO₂ capture from flue gases, while precombustion capture is implemented prior to the combustion of fuel gases and captures CO₂ from fuel gases.⁷ It should be noted that the fuel gas for precombustion CO₂ capture is usually a syngas (CO₂/H₂) produced from fossil fuels. Hydrogen in the syngas is thus purified and used as a clean fuel for gas turbines or fuel cells after precombustion CO₂ capture. In this way, power generation efficiency is increased and the emission of greenhouse gas and air pollutants is reduced. Note that the precombustion capture of CO₂ can be employed in coal-based integrated gasification combined cycle (IGCC) plants,⁸ because the fuel gas (CO₂/H₂) produced in IGCC plants normally comes out at a high pressure of (2–5 MPa) with the CO₂ concentration varying between 25 and 40 mol %.

Absorption, adsorption, membrane separation, and cryogenic separation are conventional methods used for CO₂ capture.⁹ However, the major limitations that restrict the industrial application of these methods are high cost, high energy penalty, and low separation efficiency. Recently, gas hydrate formation/decomposition has been recognized as a potential method for

CO₂ capture from fuel gas or flue gas as compared with the above-mentioned methods.^{10–15} This is because the hydrate-based separation process can produce higher CO₂ separation selectivity with lower energy costs. Since the equilibrium formation pressure of CO₂ hydrate at a given temperature is much lower than that of H₂ hydrate,¹⁶ CO₂ molecules would occupy the hydrate cavities more easily than H₂ molecules and the residual gas mixture would be a H₂-rich gas.¹⁷ However, high operation pressure is one problem that is encountered in the hydrate-based separation process for CO₂ capture from fuel gas,¹⁸ which might increase the gas compression costs while this technique is practically used in the industry.

One solution to lower the hydrate phase equilibrium pressures of fuel gas is to form gas hydrates in the presence of promoters or additives. It was found that tetrahydrofuran (THF), cyclopentane (CP), and tetra-*n*-butyl ammonium bromide (TBAB) are good candidates to reduce the phase equilibrium conditions of gas hydrates formed with the CO₂/H₂ gas mixture.^{19–22} Hashimoto et al.¹⁹ reported the phase equilibrium data of gas hydrates formed in the H₂ + CO₂ + THF mixed system. They found that the phase equilibrium pressures were greatly reduced in the presence of THF as compared with those obtained in pure water. Zhang et al.²⁰ measured the hydrate phase equilibria in the H₂ + CO₂ + CP + water system using a high-pressure differential scanning calorimeter (DSC). They reported that the hydrate formation pressures decreased significantly when adding CP into the CO₂/H₂/H₂O system. Unexpectedly, Raman spectra

Received: January 10, 2015

Revised: March 10, 2015



Table 1. Droplet Size Distributions Measured at Different Water–Oil Volume Ratios^a

	water–oil volume ratio (%)						
	10	20	30	40	50	60	70
droplet size (μm)	25.15	25.24	26.41	27.72	29.66	32.39	36.98

^aCarried out at room temperature and 0.1 MPa.

measurement indicated that H_2 would compete with CO_2 to occupy the small cages of the structure II hydrates in the presence of THF. The results of macroscopic investigations on CO_2 capture from fuel gases confirmed that the use of promoters would compromise CO_2 recovery, rate of hydrate formation, and gas uptake during the process of gas hydrate formation.^{13,23} Therefore, a better understanding of the formation kinetics of gas hydrates formed with the CO_2/H_2 gas mixture in the presence of thermodynamic or kinetic additives is needed to promote the industrial application of the hydrate-based separation process for precombustion CO_2 capture.

The performance of the hydrate-based separation process for CO_2 capture is usually evaluated by the kinetic metrics such as the hydrate selectivity of CO_2 , rate of hydrate formation, and gas consumption (gas uptake). Stirred tank reactors were preferentially employed to increase the rate of hydrate formation and gas uptake on a laboratory scale because vigorous stirring is able to enhance heat and mass transfer in the process of hydrate nucleation. The drawbacks of this arrangement are the agglomeration of gas hydrates at the interface of bulk phases and the high energy consumption on the mechanical agitation,²⁴ so the transport of hydrate-forming gases to the reaction interface might be hindered with the accumulation of gas hydrates and thus the growth of gas hydrates is interrupted. Therefore, the water conversion to gas hydrates obtained in stirred tank reactors is considerably low. One solution of this problem is to enlarge the gas/liquid contact surface using porous media instead of the contents agitation. Linga et al.²⁵ compared the kinetics of hydrate formation in a fixed sand bed and in a stirred reactor. They found that the rates of hydrate formation and water conversion to gas hydrates were enhanced in the fixed bed of silica sand. Babu et al.²⁶ assessed the performance of silica sand and silica gels for CO_2 capture from fuel gas using gas hydrate formation. They obtained a higher water conversion in the fixed bed of silica sand as compared to that in silica gels under the same conditions. Recently, it was found that gas hydrate formation was greatly enhanced in water-in-oil (W/O) emulsions as compared to that in stirred reactors using the bulk liquid,²⁷ but the mechanism of how the W/O emulsions promoted the growth of gas hydrates is still unknown. It is argued that the increased gas/liquid contact surface and gas solubility in W/O emulsions might be the main reason for the enhancement of hydrate growth.

In order to understand the mechanism of hydrate formation in water-in-oil (W/O) emulsions and promote the hydrate-based separation process for precombustion CO_2 capture, we focused on the kinetics of hydrate formation in water-in-oil emulsions for CO_2 capture from a model fuel gas (40 mol % CO_2/H_2) in this work. The purpose of this work is to evaluate the performance of the hydrate-based separation process for precombustion capture of CO_2 using W/O emulsions. The impacts of water–oil volume ratio (WOR) as well as the pressure on CO_2 separation efficiency and rate of hydrate growth were investigated. The W/O emulsions were produced by a combination of mineral oil, water, surfactant (Span 80), and cyclopentane (CP) and was employed for precombustion CO_2 capture for the first time.

2. EXPERIMENTAL SECTION

2.1. Materials. The fuel gas employed was a CO_2/H_2 gas mixture containing 40 mol % CO_2 and 60 mol % H_2 . It was used as a model gas for the typical fuel gas produced in IGCC power plants and was supplied by Chongqing Rising Gas with a reported uncertainty in the composition of ± 0.05 mol %. The industrial mineral oil (No. 7) was supplied by Shanghai Refinery with a reported viscosity of 6.6 cP at 40 °C and a density of 0.82 g/cm³. Sorbitan monooleate (Span 80) and cyclopentane (CP) were purchased from Chongqing Oriental Chemical Co., Ltd., with a certified mass purity of 99%. Span 80 is a nonionic surfactant and a lipophilic emulsifier, so the water-in-oil emulsions were produced in the presence of Span 80. Cyclopentane was used as a promoter to decrease the hydrate phase equilibrium conditions. The preparation and properties of the W/O emulsion were reported in detail elsewhere.²⁷ Briefly, the size distribution of the emulsion droplets was measured using a laser particle size analyzer (Microtrac S3500, USA). The result is given in Table 1. Deionized water was used in all experimental runs.

2.2. Apparatus. A detailed description of the experimental apparatus was presented previously in the literature.²⁸ Briefly, it consists of a high-pressure stainless steel vessel immersed in a water bath. The internal volume of the vessel was 600 cm³, and the maximum operation pressure was 10 MPa. A speed-adjustable electromagnetic stirrer was inserted into the vessel for solution agitation. Two platinum resistance thermometers with an uncertainty of 0.1 K were used to measure the gas and liquid temperature. A pressure transducer (Yokogawa Electric Corporation, Tokyo, Japan) with an uncertainty of 0.06% in the range of 0–10 MPa was used to measure the pressure of the gas phase. The temperature and pressure inside the reactor were collected by a data acquisition unit (Agilent 34970A, USA) and transferred to a computer simultaneously. A gas chromatograph (GC-2014, Shimadzu Corporation, Kyoto, Japan) with an uncertainty of 0.1 mol % was used to determine the composition of the gas mixtures at the end of the experiments.

It should be noted that, if the apparatus is scaled up for industrial use, a safety valve must be installed on the high-pressure vessel. It will operate and depressurize the system promptly once the pressure in the vessel exceeds the rated value. Therefore, the hydrate-based precombustion CO_2 capture system can be protected from the overpressure events.

2.3. Procedures. The experiments were performed in batch operation, and the procedure is given as follows. Prior to the experiments, the vessel was cleaned with deionized water and dried, and the W/O emulsion of ~ 260 cm³ was filled in the vessel (the volume ratio of water to CP was 10:1). The amount of water added in the W/O emulsions is given in Table 2. The vessel and tubing were purged with the fuel gas thrice to remove the air remaining in the system. Once the temperature and pressure in the vessel achieved the desired values, the inlet and outlet valves of the vessel were closed to separate the vessel from the gas cylinder. Then, the electromagnetic stirrer was started at a constant speed of 150 rpm. This was considered to be time zero for hydrate formation experiments. At the same time, the temperature and pressure were collected by the data acquisition unit and logged into the computer every 10 s. When the temperature restored to about 274.2 K and the pressure drop in the vessel was not observed for at least 2 h, it was considered as the end of the experiment. The composition of the gas mixtures remaining in the vessel and released from gas hydrates was measured by the gas chromatograph (GC). To obtain reproducible results, three parallel experiments were performed under each experimental condition following this procedure.

2.4. Calculation of the Amount of Gas Mixture Consumed. Based on the gas compositions measured at the beginning and end of the

Table 2. Experimental Conditions and Results for CO₂ Capture from Fuel Gas Using Hydrate Formation in Water-in-Oil Emulsions^a

exp. no.	P_{exp} (MPa)	WOR ^b (%)	liquid water (cm ³)	t_{ind} (min)	time (h)	gas uptake (mmol of gas/mol of water)	$x_{\text{CO}_2}^{\text{gas}}$ (mol %)	$x_{\text{CO}_2}^{\text{H}}$ (mol %)	R_{CO_2} (%)	S.F.
1	3.0	20	41	7	18	41.4	26.2	71.3	48.5	11.1
2				6	17	37.8	26.1	73.5	47.8	13.2
3				6	14	39.2	24.7	74.7	50.9	34.3
4	3.0	30	57	14	14	25.8	26.5	78.1	46.3	14.6
5				14	15	26.7	24.6	79.3	50.6	20.9
6				12	17	28.8	23.9	79.6	53.1	25.2
7	3.0	70	100	22	21	18.4	22.0	84.1	58.0	28.8
8				18	27	17.1	22.0	84.3	57.2	46.0
9				13	23	18.1	22.5	84.1	56.3	35.6
10	4.5	70	100	8	18	26.5	22.6	71.5	56.9	38.8
11				10	28	25.3	24.5	81.5	52.1	25.7
12				9	23	26.0	24.5	81.2	52.5	28.6
13	6.0	70	100	13	24	32.9	24.4	82.0	52.6	43.3
14				15	22	32.9	23.9	81.7	53.6	77.0
15				12	29	35.0	24.4	80.9	53.6	25.9

^aThe composition of the fuel gas was 40 mol % CO₂ and 60 mol % H₂. The experiments were performed at 274.2 K. ^bWater–oil volume ratio.

experiments, the number of moles of the gas mixture incorporated into the hydrate phase (gas consumption) was calculated by the following equation

$$\Delta n_{\text{H}} = n_{\text{g},0} - n_{\text{g},t} = \left(\frac{PV}{ZRT} \right)_0 - \left(\frac{PV}{ZRT} \right)_t \quad (1)$$

where $n_{\text{g},0}$ and $n_{\text{g},t}$ represent the number of moles of the gas mixture in the crystallizer at time 0 and time t , P is the pressure in the crystallizer, T is the temperature of the gas phase, V is the volume of the gas phase, and Z is the compressibility factor calculated by the Pitzer correlation for the second Virial coefficient²⁹

$$Z = 1 + B^0 \frac{P}{T} + \omega B^1 \frac{P}{T} \quad (2)$$

where the equations of Abbott were used for B^0 and B^1 .

Because the amount of water used for the preparation of the W/O emulsions was different, corresponding to different water–oil ratios (Table 2), the gas consumption (gas uptake) in each experiment should be normalized by considering the amount of water. Therefore, gas consumption obtained under different conditions can be compared using the normalized gas uptake. The equation to determine the normalized gas uptake is given in eq 3

$$\Delta n_{\text{H,normalized}} = \frac{\Delta n_{\text{H}}}{n_{\text{H}_2\text{O}}} \quad (3)$$

where Δn_{H} is number of moles of the gas mixture consumed for hydrate formation at the end of the experiment and $n_{\text{H}_2\text{O}}$ is the number of moles of water used in the experiment.

The rate of hydrate growth was customarily considered to be the rate of gas uptake and was calculated using the forward difference method as follows

$$\left(\frac{d\Delta n_{\text{H}}}{dt} \right)_t = \frac{\Delta n_{\text{H},t+\Delta t} - \Delta n_{\text{H},t}}{\Delta t}, \quad \Delta t = 10 \text{ s} \quad (4)$$

The average value of these rates (R_{av}) was calculated every 30 min as follows

$$R_{\text{av}} = \left[\frac{\left(\frac{d\Delta n_{\text{H}}}{dt} \right)_1 + \left(\frac{d\Delta n_{\text{H}}}{dt} \right)_2 + \dots + \left(\frac{d\Delta n_{\text{H}}}{dt} \right)_m}{m} \right], \quad m = 180 \quad (5)$$

2.5. Calculation of CO₂ Recovery and Separation Factor (S.F.).

CO₂ recovery (R_{CO_2}) and separation factor (S.F.) were two metrics proposed by Linga et al.¹¹ to evaluate the separation efficiency of CO₂ from fuel gas by gas hydrate formation. The CO₂ recovery (R_{CO_2}) was calculated by the following equation

$$R_{\text{CO}_2} = \frac{n_{\text{CO}_2}^{\text{H}}}{n_{\text{CO}_2}^{\text{feed}}} \times 100\% \quad (6)$$

where $n_{\text{CO}_2}^{\text{feed}}$ is the moles of CO₂ supplied into the reactor, and $n_{\text{CO}_2}^{\text{H}}$ is the moles of CO₂ incorporated into the hydrate crystals at the end of the experiments. The separation factor (S.F.) was determined as follows

$$\text{S.F.} = \frac{n_{\text{CO}_2}^{\text{H}} \times n_{\text{H}_2}^{\text{gas}}}{n_{\text{CO}_2}^{\text{gas}} \times n_{\text{H}_2}^{\text{H}}} \quad (7)$$

where $n_{\text{CO}_2}^{\text{gas}}$ and $n_{\text{H}_2}^{\text{gas}}$ are the moles of CO₂ and H₂ remaining in the gas phase at the end of the experiments. The symbol $n_{\text{H}_2}^{\text{H}}$ is the number of moles of H₂ enclathrated in the hydrate phase at the end of the experiments.

3. RESULTS AND DISCUSSION

3.1. Hydrate Formation in Water-in-Oil Emulsions.

The specific property of the W/O emulsions employed in this work

was presented in our previous work.²⁷ As reported, the W/O emulsions were able to stabilize with the water–oil volume ratio (WOR) ranging from 10% to 70%. It should be noted that the water cut range of this W/O emulsion was higher than that reported by Liu et al.,³⁰ but its performance in hydrate formation for CO₂ capture from fuel gas is unknown, so it is required that we carry out hydrate formation experiments using this W/O emulsion and evaluate its performance on CO₂ capture from the fuel gas. Table 2 shows the experimental conditions as well as the results that were obtained in the W/O emulsions. The temperature was fixed at 274.2 K. Three water–oil volume ratios (20, 30, and 70%) and three pressures (3.0, 4.5, and 6.0 MPa) were used in the experiments. Therefore, the performance of the W/O emulsions was systematically evaluated including the impacts of water–oil volume ratio and pressure on CO₂ capture from fuel gas.

Figure 1 shows the typical temperature and gas uptake profiles for the experiment performed at 3.0 MPa, 274.2 K, and WOR =

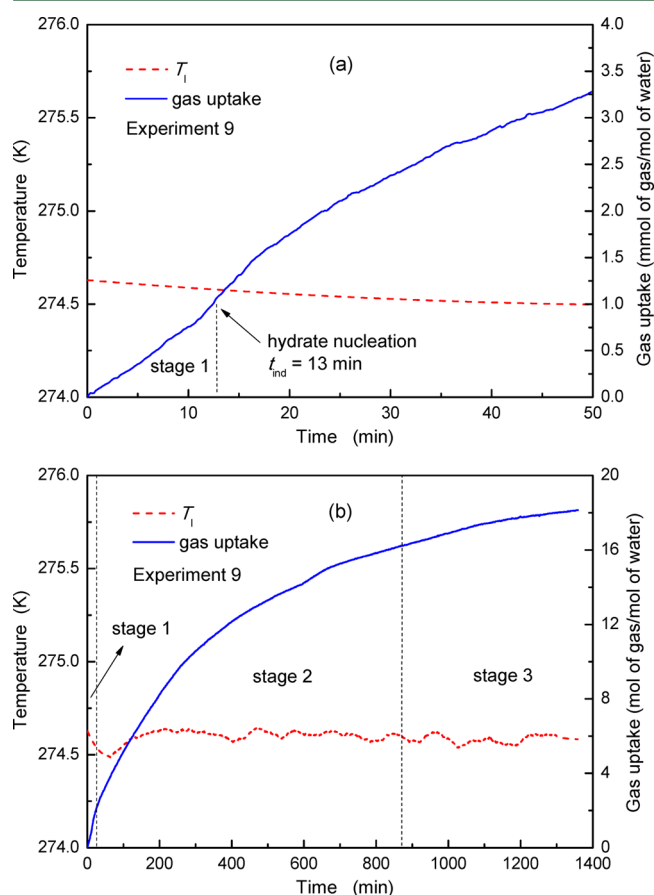


Figure 1. Temperature and gas uptake profiles for hydrate formation from the CO₂/H₂ gas mixture at 274.2 K and 3.0 MPa. The water–oil volume ratio in the W/O emulsion was fixed at 70%. (a) Enlarged temperature and gas uptake curves for hydrate formation at the first 50 min of the experiment. (b) Temperature and gas uptake curves for hydrate formation at the end of the experiment.

70% (experiment 9 in Table 2). Figure 1a shows the enlarged temperature and gas uptake curves for hydrate formation during the first 50 min, while Figure 1b shows the entire temperature and gas uptake curves that were obtained from the beginning to the end of the experiment. As can be seen in Figure 1a, the gas uptake at 13 min was observed to increase abruptly, indicating

the onset of hydrate nucleation (nucleation point). This time was identified as the induction time ($t_{\text{ind}} = 13$ min) for hydrate crystallization in the W/O emulsion. It is well-known that hydrate nucleation is usually accompanied by a sudden temperature rise in the liquid phase because of the exothermic nature of hydrate formation. Interestingly, in this case, the temperature of the liquid phase was not observed to increase at the nucleation point. One possible explanation is that the emulsified droplets (~ 37 μm in diameter, Table 1) for hydrate formation were small, and therefore, the amount of hydration heat released in the vicinity of the temperature probe was small. Thus, the temperature of the liquid phase was not observed to increase at the hydrate nucleation point. On the other hand, the gas uptake curve shown in Figure 1b can be divided into three stages (stages 1, 2, and 3). In the first stage (stage 1), the gas uptake increased slowly from time zero to the nucleation point, as can be clearly seen in Figure 1a. This stage corresponds to the phase of gas dissolution in the W/O emulsions before hydrate growth. In the second stage (stage 2), the gas uptake began to increase quickly from the nucleation point (13 min) to approximately 887 min. The gas uptake at 887 min (16.3 mmol of gas/mol of water) reached 90% of the total gas uptake. In this stage, the event of hydrate nucleation occurred and was followed by the fast growth of gas hydrates, resulting in larger gas consumption as compared to stage 1. In the third stage (stage 3), the increasing rate of gas uptake was observed to decrease and the gas uptake approached a plateau at the end of the experiment, indicating the completion of hydrate growth.

3.2. Effects of Water–Oil Volume Ratio on CO₂ Capture from Fuel Gas.

Figure 2 shows the comparison of induction

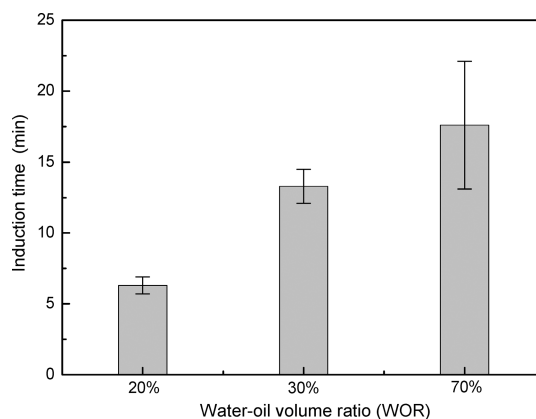


Figure 2. Comparison of the induction times obtained with the water–oil volume ratio ranging from 20% to 70%. The experiments were performed at 274.2 K and 3.0 MPa.

times for hydrate formation in W/O emulsions at different water–oil volume ratios. The experiments were carried out at 274.2 K and 3.0 MPa. It can be seen that the induction time was prolonged as the water–oil volume ratio increased from 20% to 70%. The average value for the induction times was 6, 13, and 18 min corresponding to WOR = 20, 30, and 70%. Because the emulsified droplets produced at high WORs were larger than those obtained at low WORs (Table 1), the result presented in Figure 2 indicates that hydrate nucleation in W/O emulsions occurred easily while the size of the emulsified droplets was reduced.

Figure 3 shows the impacts of water–oil volume ratio on the gas uptake obtained during the process of hydrate growth. Time

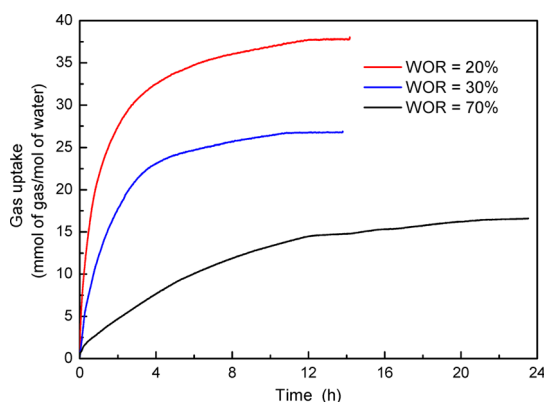


Figure 3. Effects of water–oil volume ratio on the gas uptake obtained in the process of hydrate growth. Time zero corresponds to the induction time. The experiments were performed at 274.2 K and 3.0 MPa.

zero in the figure corresponds to the nucleation point. It can be seen that the final gas uptake obtained at WOR = 20% was 38.1 mmol of gas/mol of water, which was 1.4 times larger than that obtained at WOR = 30% and 2.3 times larger than that obtained at WOR = 70%. However, it cannot be arbitrarily inferred that the W/O emulsion with WOR = 20% performed better than those with WOR = 30% and 70% only based on the value of gas uptake. As can be seen in Table 2, the CO₂ concentration in gas hydrates ($x_{\text{CO}_2}^{\text{H}}$) was 84 mol % at WOR = 70% (experiments 7–9), whereas it decreased to 73 mol % at WOR = 20% (experiments 1–3) and 79 mol % at WOR = 30% (experiments 4–6). Also, it can be seen in Figure 4 that the CO₂ recovery

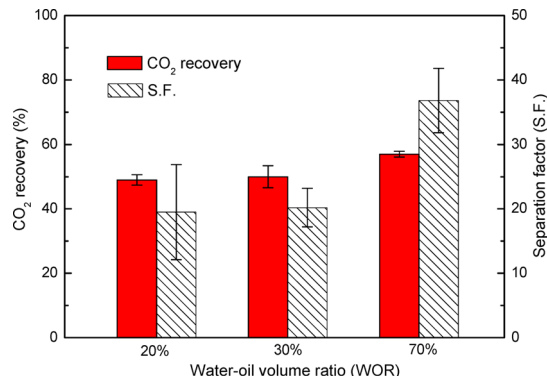


Figure 4. Effects of water–oil volume ratio on CO₂ recovery and CO₂ separation factor obtained at 274.2 K and 3.0 MPa.

(57%) and CO₂ separation factor (36.8) obtained at WOR = 70% were higher than those obtained at low WORs (20% and 30%). Therefore, it is concluded that the W/O emulsion with WOR = 70% performed better than those with WOR = 20% and 30% for CO₂ capture from fuel gas, although the gas uptake obtained at WOR = 70% was as low as 18 mmol of gas/mol of water. The reason why the normalized gas uptake at WOR = 20% was higher than those obtained at WOR = 30% and 70% is probably because the amount of water used at WOR = 20% was much smaller (41 cm³) than those used for WOR = 30% and 70% (Table 2).

In addition, it can be seen in Figure 3 that the gas uptake obtained at low WORs (20% and 30%) increased faster during the first 4 h and reached a plateau earlier than that obtained at WOR = 70%. This indicates that the process of hydrate growth at low WORs was shortened as compared with that at high WORs.

We also compared the rates of hydrate growth that were obtained at different water–oil volume ratios. The results are presented in Figure 5. As can be seen in Figure 5, during the first 4 h, the rate of

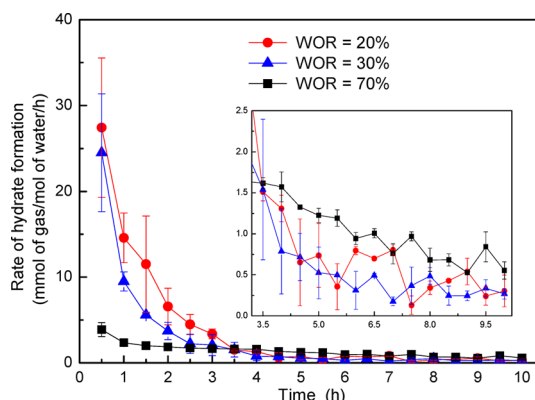


Figure 5. Comparison of the rate of hydrate growth obtained with the water–oil volume ratio ranging from 20% to 70%. Time zero corresponds to the induction time. The experiments were performed at 274.2 K and 3.0 MPa.

hydrate growth at low WORs (20% and 30%) was observed to be higher than that obtained at high WOR (70%), indicating that gas hydrates grew faster at low WORs. This is probably due to a higher amount of gas dissolved in the W/O emulsions at low WORs and the increased oil/water contact interfaces of small emulsified droplets at low WORs. Thus, the gas consumption for hydrate growth at low WORs was increased during the first 4 h. This is consistent with the results of gas uptake presented in Figure 3. Interestingly, the rate of hydrate growth at low WORs decreased substantially after 4 h and became lower than that obtained at WOR = 70%. One reason for this result is that the small droplets in the W/O emulsions with low WORs were quickly covered by hydrate films, and thus, gas transport for the following hydrate growth at the reaction interface was hindered by the thickening of the hydrate shells. Another reason is that the amount of water used in the W/O emulsions with high WOR (100 cm³ at WOR = 70%) was larger than that used for low WORs (41 cm³ at WOR = 30%, and 57 cm³ at WOR = 20%), so the process for large water droplets converting to gas hydrates was longer than the small water droplets in the W/O emulsions with low WORs.

3.3. Effects of Driving Force on CO₂ Capture from Fuel Gas. In the above experiments, we found that the optimum value for WOR was 70% among all the WORs employed in this study. Thus, the effects of pressure on CO₂ capture from fuel gas were investigated with WOR fixed at 70%. As can be seen in Table 2, the experiments (experiments 7–15) were carried out at 3.0, 4.5, and 6.0 MPa, respectively. The average value for the gas uptake obtained at 3.0, 4.5, and 6.0 MPa was 18, 26, and 34 mmol of gas/mol of water while WOR was fixed at 70%. It is well-known that the fugacity of gas components at the experiment pressure (f^{exp}) became larger with the increase of pressure, so the driving force ($f^{\text{exp}}/f^{\text{eq}} - 1$) for hydrate nucleation¹⁶ was increased at a higher pressure. Thus, the amount of gas mixture consumed for hydrate growth was increased.

The rates of hydrate growth obtained at different pressures were compared, and the results are presented in Figure 6. As can be seen in Figure 6, the rate of hydrate growth increased with the pressure increasing from 3.0 to 6.0 MPa (i.e., the driving force, $f^{\text{exp}}/f^{\text{eq}} - 1$, was increased). The average value for the rate of

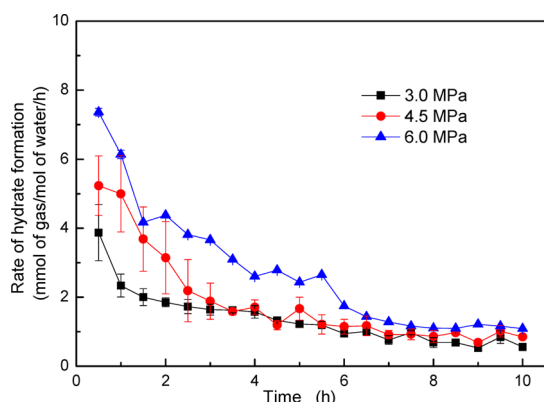


Figure 6. Effects of pressure on the rate of hydrate growth obtained at 274.2 K. The value of WOR in the W/O emulsions was fixed at 70%. Time zero corresponds to the induction time.

hydrate growth obtained 30 min after hydrate nucleation was 3.9, 5.2, and 7.4 mmol of gas/mol of water/h corresponding to 3.0, 4.5, and 6.0 MPa. In addition, the rate of hydrate growth was observed to decrease with the lapse of time at a fixed pressure. This can be explained by the fact that the diffusion of gas molecules through the hydrate shell to the hydrate/droplet interface became more difficult while the hydrate shell covering the emulsified droplets grew thicker. Also, it is interesting to note that small jumps in the rate of hydrate growth were observed at 6.0 MPa. The rates of hydrate growth obtained at 2, 4.5, and 5.5 h were higher than the adjacent points (Figure 6). At the same time, the corresponding gas uptake at 2, 4.5, and 5.5 h was observed to increase quickly (Figure 7). This can be explained by

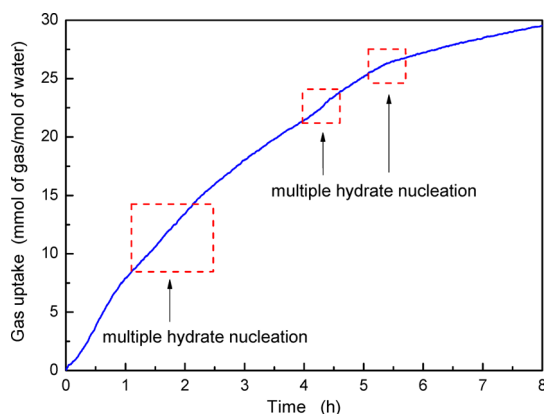


Figure 7. Gas uptake for hydrate formation in the W/O emulsions at 6.0 MPa and 274.2 K. The value of WOR in the W/O emulsions was fixed at 70%. Time zero corresponds to the induction time.

the fact that multiple hydrate nucleations on the emulsified droplets occurred as the pressure was elevated to 6.0 MPa. The occurrence of multiple hydrate nucleations in this W/O emulsion was also observed while the hydrate-forming gas mixture was changed to $\text{CH}_4/\text{N}_2/\text{O}_2$.²⁷

Figure 8 shows the impacts of pressure on CO_2 recovery (R_{CO_2}) and CO_2 separation factor (S.F.) obtained in the W/O emulsions with WOR fixed at 70%. It can be seen that the CO_2 recovery (R_{CO_2}) decreased with the increase of system pressure. The average value of CO_2 recovery (R_{CO_2}) obtained at 3.0, 4.5, and 6.0 MPa was 57, 54, and 53%, respectively. Also, the average value of separation factor decreased from 37 to 31 as the pressure

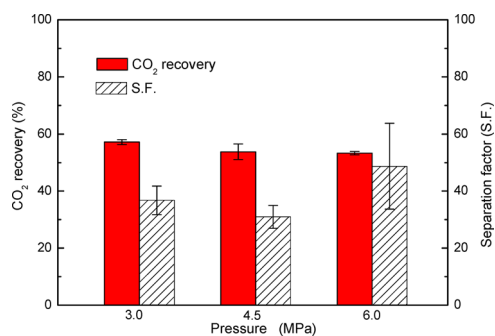


Figure 8. Effects of pressure on CO_2 recovery and CO_2 separation factor obtained in the W/O emulsions at 274.2 K. The value of WOR in the W/O emulsions was fixed at 70%.

was increased from 3.0 to 4.5 MPa. At the same time, it is noted that CO_2 concentration in the hydrate phase was 84, 78, and 81%, corresponding to 3.0, 4.5, and 6.0 MPa (Table 2). The results indicate that the selectivity of CO_2 from the fuel gas via hydrate formation in W/O emulsions decreased with the increase of operation pressure. The reason might be that more H_2 molecules were incorporated into the hydrate phase with the pressure increasing from 3.0 to 6.0 MPa. Further studies at the molecular level are needed to illustrate this mechanism. On the other hand, although the separation factor (S.F.) obtained at 6.0 MPa (48) was found to be higher than that obtained at 3.0 MPa (37), the discrepancy of the separation factor at 6.0 MPa was much larger as compared with those obtained at 3.0 and 4.5 MPa (Figure 8). This indicates that the stability of the hydrate-based separation process for CO_2 capture in the W/O emulsions decreased as the pressure was increased to a higher value. Besides, from the perspective of industrial application, a higher operation pressure will result in a significant increase in the device investment and energy costs.

3.4. Comparison of Gas Consumption for Hydrate Growth in Different Systems. Table 3 shows a summary of gas consumption for precombustion capture of CO_2 from fuel gas (40 mol % CO_2/H_2) using hydrate formation in different systems. It should be noted that the additives listed in Table 3 (CP, THF, and TBAB) were employed as promoters to reduce the hydrate phase equilibrium conditions. The gas consumption listed in the table was approximately the highest value obtained in each system. As can be seen in Table 3, for gas hydrates formed in the presence of cyclopentane (CP), the highest gas consumption obtained in this study was 39.5 mmol of gas/mol of water, which was about 18 times larger than that reported by Li et al.³¹ For gas hydrates formed in stirred reactors, the gas consumption obtained in this study (39.5 and 33.6 mmol of gas/mol of water) was also higher as compared with those obtained in the presence of THF or TBAB.^{32–34} This is because the bulk liquid water was converted to small emulsified droplets in the W/O emulsions, and thus, the gas/liquid interfacial areas were significantly increased as compared to aqueous solutions. On the other hand, it can be seen that the gas consumption obtained in the W/O emulsions was larger than that obtained in the fixed bed of silica sand in the presence of TBAB (23.43 mmol of gas/mol of water). This indicates that forming gas hydrates in W/O emulsions might be a promising option to enhance CO_2 capture from fuel gas, although the fixed bed of porous media has been proved to be more efficient than stirred reactors. However, it is noted that the gas consumption obtained in W/O emulsions cannot reach the value obtained in the fixed bed of silica sand

Table 3. Summary of Gas Consumption for Hydrate Formation from the Fuel Gas in Stirred Reactors and in the Fixed Bed of Silica Sand^a

type of promoter	concentration (mol %)	experiment format	temp (K)	pressure (MPa)	final gas consumption (mmol of gas/mol of water)
CP	1.89	STR ^b	274.2	3.0	39.5 (this work) ^c
	1.89	STR	274.2	6.0	33.6 (this work) ^d
	0.95	STR	274.65	4.0	2.2 (Li et al. ³¹)
THF	1.0	STR	279.6	4.1	8.0 (Lee et al. ³²)
	5.6	STR	$\Delta T = 4$	8.0	20 (Park et al. ³³)
	5.53	FBR ^c	279.2	6.0	51.95 (Babu et al. ³⁵)
TBAB	0.3	STR	274	3.1	20 (Xu et al. ³⁴)
	0.3	FBR	274.2	5.0	23.43 (Babu et al. ³⁵)

^aThe composition of the fuel gas was 40 mol % CO₂ and 60 mol % H₂. ^bStirred reactor. ^cObtained in W/O emulsions with water–oil volume ratio fixed at 20%. ^dObtained in W/O emulsions with water–oil volume ratio fixed at 70%. ^eFixed bed of silica sand.

while the promoter was changed to THF (51.95 mmol of gas/mol of water).³⁵ This means that the type of promoters has great impacts on hydrate growth. To increase the gas consumption and CO₂ content in the hydrate phase, the performance of W/O emulsions can be optimized via using more effective promoters in the future.

4. CONCLUSIONS

The performance of hydrate formation in W/O emulsions was investigated for the precombustion capture of carbon dioxide from fuel gas. The experiments were carried out at 274.2 K and in the pressure range of (3.0–6.0 MPa). The parameters of induction time, gas uptake, rate of hydrate growth, CO₂ recovery, and separation factor were determined to evaluate the kinetics of hydrate growth with fuel gas in the W/O emulsions. It was found that shorter induction time and higher gas uptake were obtained while the water–oil volume ratio (WOR) decreased from 70% to 20%, and gas hydrates grew faster at low WORs. However, CO₂ concentration in the hydrate phase and CO₂ recovery decreased with WOR decreasing from 70% to 20%. At a fixed WOR, higher pressure resulted in shorter induction time and higher gas uptake, whereas CO₂ concentration in the hydrate phase was reduced. The highest CO₂ content of the hydrate phase achieved 84 mol % at 3.0 MPa and WOR = 70%. The highest gas uptake obtained in the W/O emulsions was 39.5 mmol of gas/mol of water at 3.0 MPa and WOR = 20%. It was much higher than that obtained in stirred reactors in the presence of CP or THF and was comparable with that obtained in the fixed bed of silica sand in the presence of THF or TBAB. Overall, the results reported in this work indicated that the W/O emulsions can be used as a viable option to enhance hydrate formation for the precombustion capture of carbon dioxide.

■ AUTHOR INFORMATION

Corresponding Author

*Tel: +86-23-65102471. Fax: +86-23-65102471. E-mail: zhongdl@cqu.edu.cn (D.-L.Z.).

Notes

The authors declare no competing financial interest.

■ ACKNOWLEDGMENTS

The financial support from the Ministry of Education Innovation Research Team (IRT13043), the National Key Basic Research Program of China (No. 2014CB239206), and the Key Laboratory of Low-Grade Energy Utilization Technologies and Systems of Ministry of Education (No. LLEUTS-201407) is greatly appreciated.

■ REFERENCES

- (1) Keith, D. W. Why capture CO₂ from the atmosphere? *Science* **2009**, 325 (5948), 1654–1655.
- (2) Davison, J. Performance and costs of power plants with capture and storage of CO₂. *Energy* **2007**, 32 (7), 1163–1176.
- (3) Favre, E.; Bounaceur, R.; Roizard, D. A hybrid process combining oxygen enriched air combustion and membrane separation for post-combustion carbon dioxide capture. *Sep. Purif. Technol.* **2009**, 68 (1), 30–36.
- (4) Plasynski, S. I.; Litynski, J. T.; McIlvried, H. G.; Srivastava, R. D. Progress and new developments in carbon capture and storage. *Crit. Rev. Plant Sci.* **2009**, 28 (3), 123–138.
- (5) Petrakopoulou, F.; Tsatsaronis, G. Can carbon dioxide capture and storage from power plants reduce the environmental impact of electricity generation? *Energy Fuels* **2014**, 28 (8), 5327–5338.
- (6) Kanniche, M.; Gros-Bonnivard, R.; Jaud, P.; Valle-Marcos, J.; Amann, J. M.; Bouallou, C. Pre-combustion, post-combustion and oxy-combustion in thermal power plant for CO₂ capture. *Appl. Therm. Eng.* **2010**, 30 (1), 53–62.
- (7) Scheffknecht, G.; Al-Makhadmeh, L.; Schnell, U.; Maier, J. Oxy-fuel coal combustion—A review of the current state-of-the-art. *Int. J. Greenhouse Gas Control* **2011**, 5, S16–S35.
- (8) Gnanapragasam, N.; Reddy, B.; Rosen, M. Reducing CO₂ emissions from an IGCC power generation system: Effect of variations in gasifier and system operating conditions. *Energy Convers. Manage.* **2009**, 50 (8), 1915–1923.
- (9) Pires, J. C. M.; Martins, F. G.; Alvim-Ferraz, M. C. M.; Simoes, M. Recent developments on carbon capture and storage: An overview. *Chem. Eng. Res. Des.* **2011**, 89 (9), 1446–1460.
- (10) Englezos, P.; Lee, J. Gas hydrates: A cleaner source of energy and opportunity for innovative technologies. *Korean J. Chem. Eng.* **2005**, 22 (5), 671–681.
- (11) Linga, P.; Kumar, R.; Englezos, P. The clathrate hydrate process for post and pre-combustion capture of carbon dioxide. *J. Hazard. Mater.* **2007**, 149 (3), 625–629.
- (12) Li, X. S.; Xu, C. G.; Chen, Z. Y.; Wu, H. J. Tetra-n-butyl ammonium bromide semi-clathrate hydrate process for post-combustion capture of carbon dioxide in the presence of dodecyl trimethyl ammonium chloride. *Energy* **2010**, 35 (9), 3902–3908.
- (13) Li, X. S.; Xia, Z. M.; Chen, Z. Y.; Yan, K. F.; Li, G.; Wu, H. J. Gas hydrate formation process for capture of carbon dioxide from fuel gas mixture. *Ind. Eng. Chem. Res.* **2010**, 49 (22), 11614–11619.
- (14) Babu, P.; Chin, W. I.; Kumar, R.; Linga, P. Systematic evaluation of tetra-n-butyl ammonium bromide (TBAB) for carbon dioxide capture employing the clathrate process. *Ind. Eng. Chem. Res.* **2014**, 53 (12), 4878–4887.
- (15) Xu, C. G.; Chen, Z. Y.; Cai, J.; Li, X. S. Study on pilot-scale CO₂ separation from flue gas by the hydrate method. *Energy Fuels* **2014**, 28 (2), 1242–1248.
- (16) Sloan, E. D.; Koh, C. A. *Clathrate Hydrates of Natural Gases*, 3rd ed.; CRC Press: Boca Raton, FL, 2008.

- (17) Ho, L. C.; Babu, P.; Kumar, R.; Linga, P. HBGS (hydrate based gas separation) process for carbon dioxide capture employing an unstirred reactor with cyclopentane. *Energy* **2013**, *63*, 252–259.
- (18) Kumar, R.; Wu, H. J.; Englezos, P. Incipient hydrate phase equilibrium for gas mixtures containing hydrogen, carbon dioxide and propane. *Fluid Phase Equilib.* **2006**, *244* (2), 167–171.
- (19) Hashimoto, S.; Murayama, S.; Sugahara, T.; Ohgaki, K. Phase equilibria for $H_2 + CO_2$ + tetrahydrofuran + water mixtures containing gas hydrates. *J. Chem. Eng. Data* **2006**, *51* (5), 1884–1886.
- (20) Zhang, J. S.; Yedlapalli, P.; Lee, J. W. Thermodynamic analysis of hydrate-based pre-combustion capture of CO_2 . *Chem. Eng. Sci.* **2009**, *64* (22), 4732–4736.
- (21) Li, X. S.; Xia, Z. M.; Chen, Z. Y.; Yan, K. F.; Li, G.; Wu, H. J. Equilibrium hydrate formation conditions for the mixtures of $CO_2 + H_2$ + tetrabutyl ammonium bromide. *J. Chem. Eng. Data* **2010**, *55* (6), 2180–2184.
- (22) Babu, P.; Yang, T.; Veluswamy, H. P.; Kumar, R.; Linga, P. Hydrate phase equilibrium of ternary gas mixtures containing carbon dioxide, hydrogen and propane. *J. Chem. Thermodyn.* **2013**, *61*, 58–63.
- (23) Kim, S. M.; Lee, J. D.; Lee, H. J.; Lee, E. K.; Kim, Y. Gas hydrate formation method to capture the carbon dioxide for pre-combustion process in IGCC plant. *Int. J. Hydrogen Energy* **2011**, *36* (1), 1115–1121.
- (24) Linga, P.; Kumar, R.; Lee, J. D.; Ripmeester, J.; Englezos, P. A new apparatus to enhance the rate of gas hydrate formation: Application to capture of carbon dioxide. *Int. J. Greenhouse Gas Control* **2010**, *4* (4), 630–637.
- (25) Linga, P.; Daraboina, N.; Ripmeester, J. A.; Englezos, P. Enhanced rate of gas hydrate formation in a fixed bed column filled with sand compared to a stirred vessel. *Chem. Eng. Sci.* **2012**, *68* (1), 617–623.
- (26) Babu, P.; Kumar, R.; Linga, P. Pre-combustion capture of carbon dioxide in a fixed bed reactor using the clathrate hydrate process. *Energy* **2013**, *50*, 364–373.
- (27) Zhong, D. L.; Ding, K.; Lu, Y. Y.; Yan, J.; Zhao, W. L. Methane recovery from coal mine gas using hydrate formation in water-in-oil emulsions. *Appl. Energy* **2014**, DOI: 10.1016/j.apenergy.2014.11.010.
- (28) Zhong, D. L.; Sun, D. J.; Lu, Y. Y.; Yan, J.; Wang, J. L. Adsorption-hydrate hybrid process for methane separation from a $CH_4/N_2/O_2$ gas mixture using pulverized coal particles. *Ind. Eng. Chem. Res.* **2014**, *53* (40), 15738–15746.
- (29) Smith, J. M.; Van Ness, H. C.; Abbott, M. W. *Introduction to Chemical Engineering Thermodynamics*; McGraw-Hill, Inc.: New York, 2001.
- (30) Liu, H.; Wang, J.; Chen, G.; Liu, B.; Dandekar, A.; Wang, B.; Zhang, X.; Sun, C.; Ma, Q. High-efficiency separation of a CO_2/H_2 mixture via hydrate formation in W/O emulsions in the presence of cyclopentane and TBAB. *Int. J. Hydrogen Energy* **2014**, *39* (15), 7910–7918.
- (31) Li, X. S.; Xu, C. G.; Chen, Z. Y.; Cai, J. Synergic effect of cyclopentane and tetra-n-butyl ammonium bromide on hydrate-based carbon dioxide separation from fuel gas mixture by measurements of gas uptake and X-ray diffraction patterns. *Int. J. Hydrogen Energy* **2012**, *37* (1), 720–727.
- (32) Lee, H. J.; Lee, J. D.; Linga, P.; Englezos, P.; Kim, Y. S.; Lee, M. S.; Kim, Y. D. Gas hydrate formation process for pre-combustion capture of carbon dioxide. *Energy* **2010**, *35* (6), 2729–2733.
- (33) Park, S.; Lee, S.; Lee, Y.; Lee, Y.; Seo, Y. Hydrate-based pre-combustion capture of carbon dioxide in the presence of a thermodynamic promoter and porous silica gels. *Int. J. Greenhouse Gas Control* **2013**, *14*, 193–199.
- (34) Xu, C. G.; Zhang, S. H.; Cai, J.; Chen, Z. Y.; Li, X. S. CO_2 (carbon dioxide) separation from CO_2-H_2 (hydrogen) gas mixtures by gas hydrates in TBAB (tetra-n-butyl ammonium bromide) solution and Raman spectroscopic analysis. *Energy* **2013**, *59*, 719–725.
- (35) Babu, P.; Ho, C. Y.; Kumar, R.; Linga, P. Enhanced kinetics for the clathrate process in a fixed bed reactor in the presence of liquid promoters for pre-combustion carbon dioxide capture. *Energy* **2014**, *70*, 664–673.